**Ind. J. Pharm. Edu. Res., 2026; 60(3s):s1139-s1155.**
https://www.ijper.org

Original Article

# *Lentinula edodes* Polysaccharides Inhibit Estrogen Biosynthesis Enzymes in Hormone-Dependent Breast Cancer

**Chandrasekaran Ponnusamy[1], V V Sathibabu Uddandrao[2,3], Vadivukkarasi Sasikumar[1], Puniethaa Prabhu[4], Saravanan Ganapathy[1,*]**

[1]Department of Biochemistry, K.S. Rangasamy College of Arts and Science (Autonomous), Tiruchengode, Namakkal, Affiliated to Periyar University, Salem, Tamil Nadu, INDIA.
[2]Department of Biotechnology, Karpagam Academy of Higher Education (Deemed to be University), Coimbatore, Tamil Nadu, INDIA.
[3]Centre for Molecular Therapeutics, Karpagam Academy of Higher Education (Deemed to be University), Tamil Nadu, Coimbatore, INDIA.
[4]Department of Biotechnology, K.S. Rangasamy College of Technology, Tiruchengode, Namakkal, Tamil Nadu, INDIA.

## ABSTRACT

**Background / Objective:** Breast cancer, a leading cause of death among women, is closely associated with estrogen metabolism. This study investigated the potential of partially purified polysaccharides from Lentinula edodes (shiitake mushroom) as natural inhibitors of key enzymes involved in estrogen production aromatase, estrone sulfatase, and 17β hydroxysteroid dehydrogenase which are vital in the progression of hormone-dependent breast cancer. **Materials and Methods:** Polysaccharide fractions were purified using ion-exchange and size-exclusion chromatography. Enzyme inhibition was assessed through ELISA and colorimetric assays, which revealed concentration-dependent inhibition, with the highest activity observed at 400 µg/mL: aromatase (87.25%, $IC_{50}$=181.25 µg/mL), estrone sulfatase (86.62%, $IC_{50}$=187.5 µg/mL), and 17β hydroxysteroid dehydrogenase (86.67%, $IC_{50}$=208.4 µg/mL). GC-MS analysis identified 33 bioactive compounds, of which 14 were evaluated for pharmacokinetic and drug-likeness properties using SwissADME. **Results:** Molecular docking showed strong binding interactions between selected compounds (D-fructose and diethyl mercaptal pentaacetate) and the target enzymes, supporting their inhibitory potential. In silico toxicity predictions further confirmed favorable safety profiles. **Conclusion:** Collectively, these findings highlight L. edodes-derived polysaccharides and associated bioactive molecules as promising natural inhibitors of estrogen biosynthesis, offering new perspectives for therapeutic strategies against hormone-dependent breast cancer.

**Keywords:** *Lentinula edodes*, Breast Cancer, Natural products, Estrogen biosynthesis Enzymes.

**Correspondence:**
**Dr. Saravanan Ganapathy**
Assistant Professor and Head, Department of Biochemistry, K.S. Rangasamy College of Arts and Science (Autonomous), Tiruchengode, Namakkal-637215, Tamil Nadu, INDIA.
Email: sarabioc@gmail.com

**Received:** 11-02-2026;
**Revised:** 05-03-2026;
**Accepted:** 28-04-2026.

## INTRODUCTION

Breast cancer is the most frequently detected cancer among women globally and is the primary cause of cancer-related death. The occurrence of this condition is continuously increasing, with the death rate in Southeast Asia projected to rise by 61.7% by the year 2040.[1] According to predictions,[2] by 2025, the number of disability-adjusted life years caused by female breast cancer in India is expected to reach 5.6 million. Early mortality accounts for 5.3 million of these disability-adjusted life years, with disability accounting for the remaining years. The age-standardized incidence of breast cancer in Indian women has risen significantly between 1990 and 2016, with a similar trend observed worldwide over the past 26 years.[3] Estrogen, especially 17β-estradiol (E2), is essential in Hormone-Dependent Breast Cancer (HDBC), with elevated levels detected in breast tumors compared to plasma. The key enzymes involved in estrogen biosynthesis aromatase, Estrone Sulfatase (ES), and 17β hydroxysteroid dehydrogenase (17βHSD) are engaged in converting androgens to estrogens, as well as promoting estrone conversion to E2, which stimulates tumor cell proliferation.[4] Extended estrogen exposure, which is affected by factors such as the timing of menopause, the age at which a woman has her first child, and the total number of years of childbearing, increases the likelihood of developing breast cancer. Thus, targeting estrogen biosynthesis through enzyme inhibition is a promising strategy for treating hormone-dependent breast cancer.[5]

*Lentinula edodes* (*L. edodes*) has a broad range of biological functions that greatly benefit human health. These functions

**DOI:** 10.5530/ijper.20263074

include strong anticancer, antitumor, and antimicrobial effects, as well as significant anticaries activity. It also shows anti-atherosclerotic, antioxidant, and antidiabetic properties, protectively contributing to liver health. Moreover, *L. edodes* helps to regulate cholesterol levels, modulate immune responses, and enhance the overall immune system. Its capacity to lower homocysteine levels further supports heart health.[6] Its bioactive polysaccharides exhibit significant free radical scavenging activity, positioning them as promising natural antioxidants. With increasing concerns over the adverse effects of synthetic antioxidants, organic substitutes are of growing interest. However, challenges in extraction and chemical characterization have hindered the broader application of *L. edodes* polysaccharides.[7,8] This research investigates, for the first time, the potential of *L. edodes* polysaccharides and other bioactive compounds as HDBC inhibitors via molecular docking. We hypothesize that these polysaccharides may inhibit estrogen biosynthesis pathways, providing a natural strategy for breast cancer prevention. The inhibitory effects of partially purified Polysaccharides from *L. edodes* (PLE) on key enzymes involved in estrogen biosynthesis aromatase, ES, and 17βHSD, using molecular docking studies to evaluate binding affinities and interaction profiles with the target enzymes.

## MATERIALS AND METHODS

### Collection and Preparation of Samples

*L. edodes*, an edible mushroom, was obtained from the TNAU in Coimbatore, Tamil Nadu. The fruiting bodies of *L. edodes* were rinsed and then freeze dried at temperatures ranging from -40 to -50°C. Once dried, the mushrooms were ground into fine particles, sifted, and kept in a sealed box in the deep freeze at -20°C for later investigation.

### Extraction of Partially Purified Polysaccharides from *L. edodes*

To assess the bioactivity of polysaccharides, the extraction method was optimized to ensure efficacy. In this study, 50 g of air-dried, powdered cap tissue was extracted with a chloroform: methanol: water mixture (200:200:60, v/v/v). The residue was then autoclaved with 500 mL of distilled water at 121°C for 1 hr. Following thermal extraction, the solution was filtered, and the extract was concentrated under reduced pressure at 40°C. Cold ethanol was slowly added to the concentrate to induce precipitation. The mixture was centrifuged at 6026×g for 20 min, and the resulting precipitate was carefully collected.

### Isolation of Partially Purified Polysaccharides Utilizing Ion Exchange Chromatography and Size-Exclusion Chromatography

Ion Exchange Chromatography (IEC) was performed using a Diethylaminoethyl (DEAE) cellulose column (5×30 cm; Sigma Chemical Co., St. Louis, MO, USA) pre-equilibrated with 10 mM Tris-HCl buffer (pH 7.4). Polysaccharides retained on the column were eluted at a flow rate of 0.2 mL/min with a stepwise NaCl gradient (0, 0.1, 0.5, and 1 M). Eluted fractions were monitored at 620 nm, pooled, and freeze-dried. Further purification was carried out by Size-Exclusion Chromatography (SEC) using a Sephadex G-25 column (5×30 cm), pre-equilibrated with the same buffer. Elution conditions in SEC were identical to those used in IEC, and all procedures were conducted at 4°C. Fractions showing absorbance at 620 nm were combined and lyophilized for subsequent analysis.

### Aromatase Inhibitory Activity

The effect of PLE on human aromatase was evaluated using a commercial Human Aromatase ELISA Kit (Cat. No: EEL021, Invitrogen, India), following the manufacturer's instructions. Briefly, samples (100-400 µL) were incubated in antibody-coated plates, and enzyme activity was quantified colorimetrically at 450 nm. The assay included blank, negative control, and four PLE-treated groups. Percentage inhibition was calculated using the formula: Inhibition (%) = (1-Corrected OD_sample / Corrected OD_negative control) × 100.

### Estrone Sulfatase (ES) Inhibition Activity

ES activity was determined using a sulfatase assay kit (Cat. No: EIA17E3S, Invitrogen, India) based on the hydrolysis of a sulfate ester to 4-nitrocatechol, measured at 515 nm. Standards (0-50 nmol/well) were prepared, and PLE samples (100-400 µL) were incubated with substrate at 37°C. Absorbance was recorded at 515 nm, and inhibition was calculated as described above.

### 17βHSD Inhibition Activity

The effect of PLE on mouse 17βHSD was assessed using a commercial ELISA kit (Cat. No. EH2RB, Invitrogen, India). Samples (100-400 µL mixed with diluent) were incubated and enzyme activity was measured at 450 nm. Blank, negative control, and four PLE-treated groups were included, and inhibition was calculated using the same formula.

### Gas Chromatography Mass Spectrophotometry (GC-MS) Analysis

GC-MS analysis of PLE was performed according to the method of Uddandrao *et al.*[8] The mass spectra of the separated compounds were compared against the National Institute of Standards and Technology (NIST) library database for the identification of bioactive constituents.

### Retrieval of GC-MS Compound Data

Compounds identified through GC-MS analysis were selected for computational evaluation. Their SMILES representations were retrieved from the PubChem database using compound names or CAS numbers. The corresponding 3D structures were

downloaded in SDF format and subsequently converted to PDB format for further molecular modeling analyses.

### Prediction of PLE bioactive compound toxicity

The toxicity of bioactive compounds was evaluated using Toxicity Predictor 3.0,[9] an in-silico tool based on QSAR models and machine learning algorithms. Thirty-one compounds identified from PLE by GC-MS were analyzed. To estimate $LD_{50}$ values and assign toxicity classes according to the Globally Harmonized System (GHS), the chemical structures were retrieved from the PubChem database in SMILES format and submitted to the predictor.

### Pharmacokinetics and Drug-Likeness Analysis

A total of 33 selected compounds were subjected to pharmacokinetic and drug-likeness evaluation using the SwissADME web server (http://www.swissadme.ch/).[10] The SMILES notation of each compound was uploaded into SwissADME to predict key drug-likeness parameters, including Lipinski's Rule of Five, Ghose filter, Veber's rule, and Egan's rule. Pharmacokinetic characteristics were also examined, including cytochrome P450 inhibition potential, blood-brain barrier permeability, and gastrointestinal absorption. The obtained data were systematically recorded for further interpretation and screening of potential bioactive candidates.

### Preparation of Protein Structure

The 3D structures of aromatase (3EQM), ES (8EG3), and 17βHSD (1BHS) were obtained from the Protein Data Bank. The protein structures were preprocessed by removing non-essential molecules, adding hydrogens, and assigning Gasteiger charges using UCSF Chimera. Missing residues were modeled with Modeller. AutoDock Tools was used to switch the proteins and ligands to the PDBQT format for docking analysis. The affinity grid maps were optimized to ensure accurate docking within the active sites of each enzyme (Table 1).

### Molecular Docking Investigations

Molecular docking was performed using AutoDock4 (v4.0.1) and the Lamarckian genetic algorithm, with 50 docking runs, a population size of 200, and energy evaluations of 7 and 2.5 million. Parameters included a translation step of 2.0 Å, a mutation rate of 0.02, a crossover rate of 0.8, and an RMSD clustering threshold of 2.0 Å. Additionally, AutoDock Vina was used with a completeness parameter of 8, generating the top nine binding modes ranked by binding affinity. Post-docking analysis involved converting output files to PDB format using Open Babel for visualization in PyMOL, where hydrogen bonds, hydrophobic interactions, and ligand orientation were examined. LigPlot+ was used to generate 2D interaction maps. Utilizing AutoDock4, the estimated inhibition constant (Ki) values were calculated, and the pKm values were determined via log (1/Km). The final docking poses were analyzed in PyMOL to understand ligand-protein interactions.

## RESULTS

### Chromatographic Profiles of Polysaccharide Purification

Polysaccharides were first isolated through IEC using a stepwise NaCl gradient ranging from 0.0 M to 1.0 M, while monitoring the eluted fractions at 620 nm to evaluate carbohydrate levels (Figure 1A). Distinct peaks were observed at various salt concentrations, signifying the existence of polysaccharide subpopulations with different charge properties. The five fractions with the highest absorbance at NaCl concentrations of 0.0, 0.1, 0.5, and 1.0 M were combined and further purified using SEC. The SEC elution profile displayed a significant peak spanning from fractions 7 to 18, with the highest absorbance recorded between fractions 10 and 15, indicating a substantial high-molecular-weight polysaccharide population. The carbohydrate content of the fractions was evaluated at a wavelength of 620 nm (Figure 1B). The integrated IEC and SEC findings suggest that the extracted polysaccharides consist of heterogeneous components that vary in both charge and molecular size, highlighting the complexity of the original polysaccharide mixture.

### Aromatase Inhibition

PLE demonstrated a noticeable dose-dependent inhibition, achieving a peak of 87.25% at a concentration of 400 µg/mL, which is marginally higher than the positive control (Figure 2A). A strong reduction of aromatase activity was shown by the $IC_{50}$, which was found to be 181.25 µg/mL.

### ES Inhibition

A concentration-dependent effect was noted, with the maximum inhibition reaching 86.62% at 400 µg/mL (Figure 2B). The estimated $IC_{50}$ value was around 187.5 µg/mL, highlighting the strong inhibition of ES activity by PLE.

**Table 1: Docking grid parameters used for molecular docking simulations of PLE-derived bioactive compounds with target proteins.**

| Protein | PDB ID | Grid Dimensions (Å) | Spacing (Å) | Grid Center Coordinates (x, y, z) |
|---|---|---|---|---|
| Aromatase | 3EQM | 126 × 100 × 106 | 1.000 | (51.94, 44.63, 46.42) |
| ES | 8EG3 | 126 × 94 × 78 | 1.000 | (50.62, -7.80, 26.93) |
| 17βHSD | 1BHS | 70 × 60 × 70 | 1.000 | (16.00, 2.00, 1.00) |

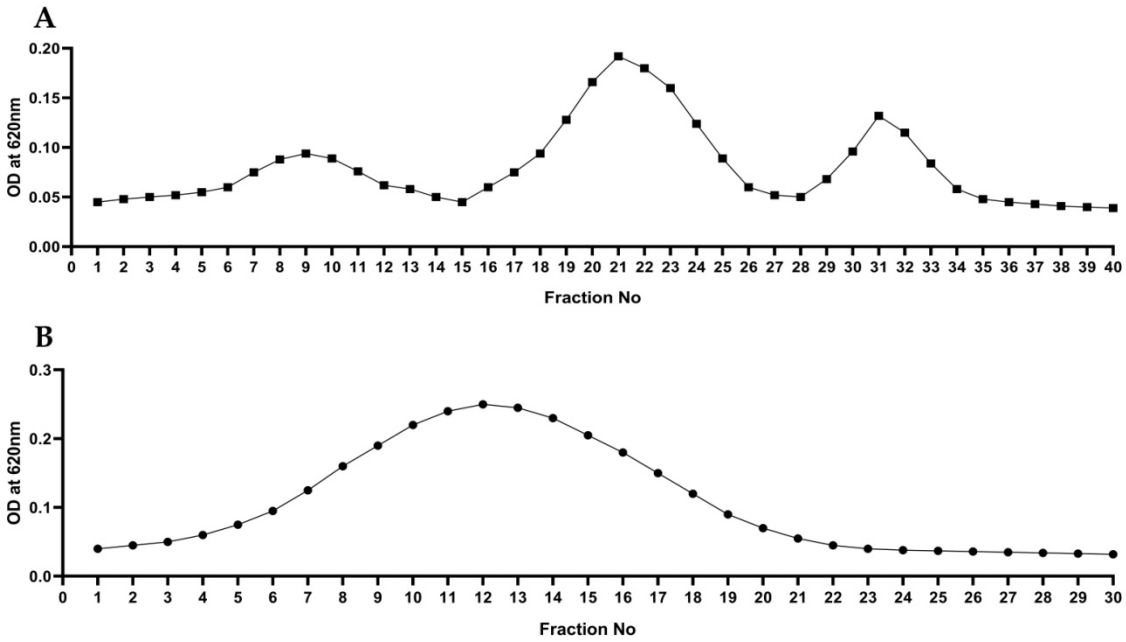


**Figure 1:** Polysaccharide elution profiles obtained during purification of *PLE*. (A) Ion-exchange chromatography (IEC) performed on a DEAE-Sepharose column with stepwise elution using NaCl gradients ranging from 0.0-1.0 M; polysaccharide fractions were detected at 620 nm using the phenol-sulfuric acid method. (B) Size-exclusion chromatography (SEC) of pooled IEC fractions carried out on a Sephadex G-100 column, with polysaccharide elution monitored at 620 nm.

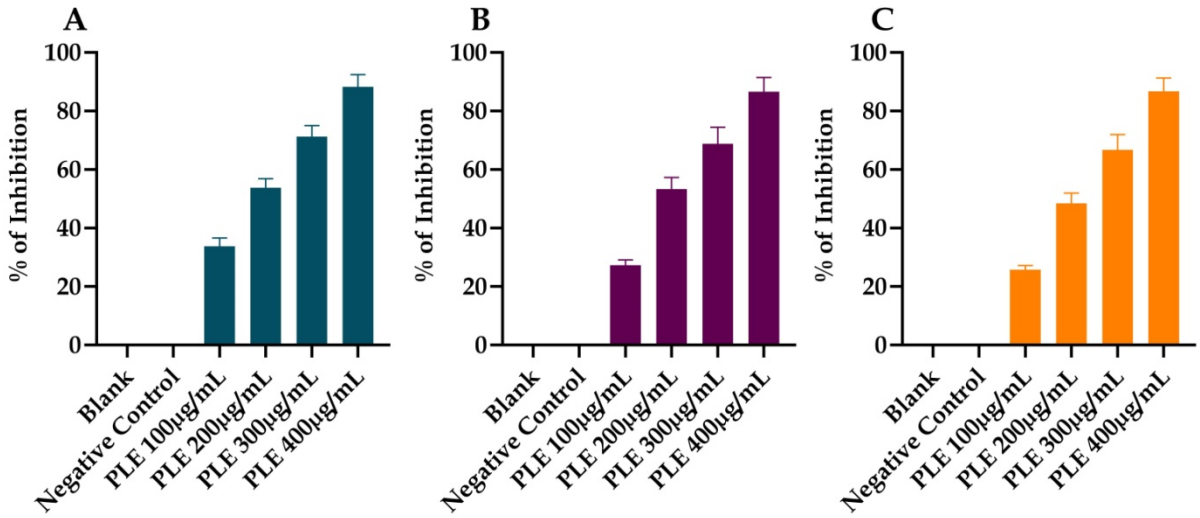


**Figure 2:** Inhibitory effects of PLE on estrogen biosynthesis enzymes. Enzyme inhibition was measured using *in vitro* assays with increasing concentrations of PLE (100-400 µg/mL). PLE caused a dose-dependent suppression of (A) aromatase activity, (B) estrone sulfatase (ES) activity, and (C) 17β-hydroxysteroid dehydrogenase (17β-HSD) activity. Activities were quantified spectrophotometrically and are expressed as percentage inhibition relative to untreated controls. Data are presented as Mean±SD from three independent experiments (*n*=3).

## 17βHSD Inhibition

PLE exhibited a gradual increase in inhibition, peaking at 86.67% at 400 µg/mL (Figure 2C). The $IC_{50}$ was approximated to be 208.35 µg/mL, confirming its potential to inhibit 17βHSD and affect estrogen metabolism.

## Profiling of Bioactive Compounds in PLE Using GC-MS

GC-MS analysis of the PLE identified 33 bioactive compounds, which was confirmed by comparing the mass spectra with the NIST database. The identification process used retention time, peak area, and spectral matching from the Total Ion Chromatogram, with 33 distinct peaks observed in the chromatogram (Figures 3, 4 and Table 2).

**Table 2: GC-MS analysis of bioactive compounds in PLE and list of each identified compound with its retention time, chemical name, PubChem CID, and SMILES notation, providing a comprehensive chemical profile of the extract.**

| Retention Time | Name | Pub Chem CID | SMILES |
|---|---|---|---|
| 3.01 | D-Fructose, diethyl mercaptal, pentaacetate | 344472 | CCSC(COC(=O)C)(C(C(C(COC(=O)C)OC(=O)C)OC(=O)C)OC(=O)C)SCC |
| 4.36 | L-Glucose | 10954115 | C([C@@H]([C@@H]([C@H]([C@@H](C=O)O)O)O)O)O |
| 5.09 | Alpha-d-xylopyranose | 6027 | C1[C@H]([C@@H]([C@H]([C@H](O1)O)O)O)O |
| 5.92 | L-Glutamine | 5961 | C(CC(=O)N)[C@@H](C(=O)O)N |
| 5.93 | Pentane-1,2,3,4,5-pentaol | 6912 | C([C@H](C([C@H](CO)O)O)O)O |
| 6.66 | D-Mannotetradecane-1,2,3,4,5-pentaol | 552347 | CCCCCCCCCC(C(C(C(CO)O)O)O)O |
| 7.52 | L-Gala-l-ido-octonic lactone | 219893 | C(C(C(C(C1C(C(C(=O)O1)O)O)O)O)O)O |
| 8.48 | L-Glutamine | 5961 | C(CC(=O)N)[C@@H](C(=O)O)N |
| 8.84 | d-Glucoheptose | 76599 | C([C@H]([C@H]([C@@H]([C@H]([C@H](C=O)O)O)O)O)O)O |
| 9.59 | Melezitose | 92817 | C([C@@H]1[C@H]([C@@H]([C@H]([C@H](O1)O[C@H]2[C@@H]([C@H](O[C@@]2(CO)O[C@@H]3[C@@H]([C@H]([C@@H]([C@H](O3)CO)O)O)O)CO)O)O)O)O)O |
| 10.42 | Maltose | 6255 | C([C@@H]1[C@H]([C@@H]([C@H]([C@H](O1)O[C@@H]2[C@H](O[C@H]([C@@H]([C@H]2O)O)O)CO)O)O)O)O |
| 10.44 | d-Glycero-d-tallo-heptose | - | - |
| 10.48 | Xylitol | 6912 | C([C@H](C([C@H](CO)O)O)O)O |
| 11.51 | Galactitol | 11850 | C([C@H]([C@@H]([C@@H]([C@H](CO)O)O)O)O)O |
| 13.41 | DL-Arabinitol | 94154 | C([C@H](C([C@@H](CO)O)O)O)O |
| 14.17 | Ribitol | 6912 | C([C@H](C([C@H](CO)O)O)O)O |
| 15.59 | Inositol, 1-deoxy- | 101715 | C1C(C(C(C(C1O)O)O)O)O |
| 16.00 | 1-Deoxy-d-mannitol | 121864 | C(CC(=O)N)[C@@H](C(=O)O)NC[C@H]([C@H]([C@@H]([C@@H](CO)O)O)O)O |
| 16.41 | Pentadecanoic acid | 13849 | CCCCCCCCCCCCCCC(=O)O |
| 17.35 | D-glycero-D-manno-Heptitol | 441439 | C([C@H]([C@H](C([C@@H]([C@@H](CO)O)O)O)O)O)O |
| 18.29 | L-Glucose | 10954115 | C([C@@H]([C@@H]([C@H]([C@@H](C=O)O)O)O)O)O |
| 19.25 | á-d-Lyxofuranoside, O-nonyl- | - | - |
| 20.47 | 1,5-Anhydroglucitol | 64960 | C1[C@@H]([C@H]([C@@H]([C@H](O1)CO)O)O)O |
| 22.51 | D-Gluconic acid, γ-lactone | 92283 | C(=O)[C@@H]([C@@H]1[C@@H]([C@@H](C(=O)O1)O)O)O |
| 22.57 | α-Sedoheptitol | 441439 | C([C@H]([C@H](C([C@@H]([C@@H](CO)O)O)O)O)O)O |
| 23.52 | cis-Vaccenic acid | 5282761 | CCCCCC/C=C\CCCCCCCCCC(=O)O |
| 25.01 | n-Hexadecanoic acid | 985 | CCCCCCCCCCCCCCCC(=O)O |
| 25.77 | Octadecanoic acid | 5281 | CCCCCCCCCCCCCCCCCC(=O)O |
| 25.84 | d-Mannose | 18950 | C([C@@H]1[C@H]([C@@H]([C@@H](C(O1)O)O)O)O)O |
| 25.90 | d-Gulopyranose | 441033 | C([C@@H]1[C@@H]([C@H]([C@H](C(O1)O)O)O)O)O |
| 26.38 | Oleic Acid | 445639 | CCCCCCCC/C=C\CCCCCCCC(=O)O |
| 27.33 | L-Ascorbic acid, 6-octadecanoate | 54725318 | CCCCCCCCCCCCCCCCCC(=O)OC[C@@H]([C@@H]1C(=C(C(=O)O1)O)O)O |
| 28.29 | Galacto-heptulose | 5459879 | C([C@H]([C@H]([C@H]([C@@H](C(=O)CO)O)O)O)O)O |

## Toxicity profile of the bioactive compounds

The predicted toxicity profiles (Table S1-S4) of 31 bioactive compounds derived from PLE indicated that 74.2% (Figure 5) were categorized as relatively non-toxic (Toxicity Class 6, $LD_{50}$ > 5000 mg/kg). One compound was classified as Class 5 (low toxicity), five as Class 4 (moderate toxicity), one in Class 3, and two as Class 2 (higher toxicity). These results imply that most of compounds exhibit a favorable safety profile, which supports their potential applications in pharmaceuticals or nutraceuticals.

## Assessment of Drug-Likeness and Pharmacokinetics

In the bioactive compounds identified in PLE, 14 compounds were selected for molecular docking studies due to their promising Absorption, Distribution, Metabolism, and Excretion (ADME) and drug-likeness profiles. Table 3 lists these identified compounds' pharmacokinetic properties, and Table 4 shows the assessments of their oral bioavailability and drug-likeness. The majority of the compounds exhibited favorable pharmacokinetic characteristics pharmacokinetic characteristics were demonstrated by the majority of the compounds, ranging from low permeability across the blood-brain barrier, good gastrointestinal absorption, and no discernible inhibition of important cytochrome P450 enzymes. The ADME assessment also indicated good water solubility and bioavailability scores for most of the compounds, indicating that they are suitable for systematic circulation.

## Inhibition of Estrogen Biosynthesis Key Enzymes by PLE

Pharmacokinetic assessments and drug-likeness evaluations of bioactive substances extracted from PLE resulted in the identification of 14 promising candidates. These compounds were tested for their inhibitory effects on three major enzymes involved

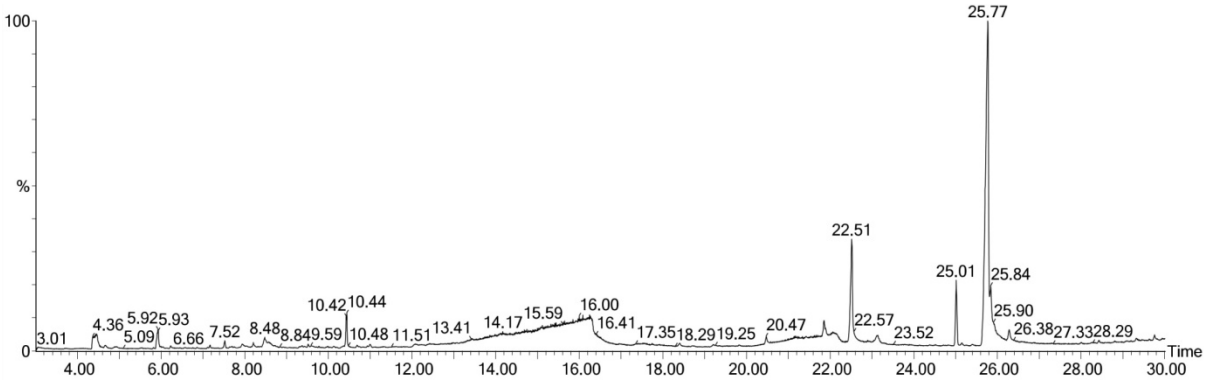


**Figure 3:** GC-MS total ion chromatogram of the PLE. The analysis revealed 33 distinct peaks, each corresponding to a bioactive compound. Identification was achieved by comparing retention times, peak areas, and mass spectra with the NIST database, confirming the presence of diverse phytoconstituents in the extract. The chromatogram provides an overview of the compound distribution and relative abundance within PLE.

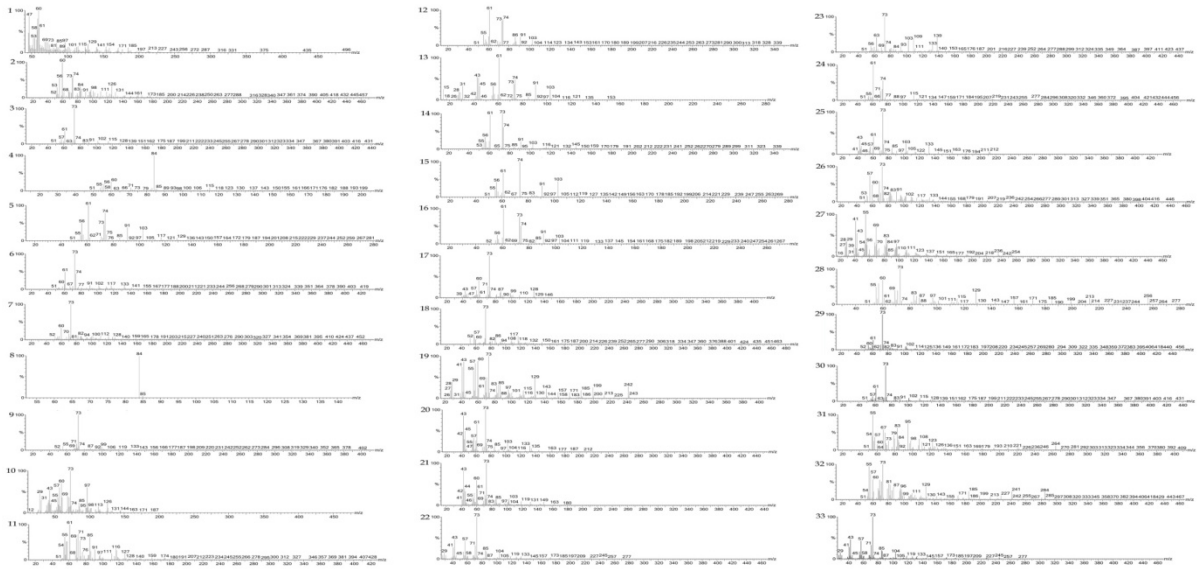

**Figure 4:** Representative gas GC-MS spectra of selected bioactive compounds identified in the PLE. The mass spectra were matched with reference spectra from the NIST database, confirming compound identity based on retention time, fragmentation patterns, and spectral similarity. These spectra illustrate the structural diversity of PLE constituents revealed by GC-MS analysis.

**Table 3: Predicted pharmacokinetic properties of selected bioactive compounds from PLE as determined using SwissADME. Properties include Absorption, Distribution, Metabolism, and Excretion (ADME) parameters relevant for evaluating drug-likeness and oral bioavailability.**

| Pub Chem CID | GI absorption | BBB permeant | P-gp substrate | CYP1A2 inhibitor | CYP2C19 inhibitor | CYP2C9 inhibitor | CYP2D6 inhibitor | CYP3A4 inhibitor | Log$K_p$ (skin permeation) |
|---|---|---|---|---|---|---|---|---|---|
| 344472 | Low | No | Yes | No | Yes | No | Yes | No | -7.99 cm/s |
| 10954115 | Low | No | No | No | No | No | No | No | -9.49 cm/s |
| 6027 | Low | No | No | No | No | No | No | No | -9.36 cm/s |
| 5961 | High | No | No | No | No | No | No | No | -9.43 cm/s |
| 6912 | Low | No | No | No | No | No | No | No | -8.99 cm/s |
| 552347 | High | No | No | No | No | No | No | No | -6.88 cm/s |
| 219893 | Low | No | Yes | No | No | No | No | No | -10.07 cm/s |
| 76599 | Low | No | No | No | No | No | No | No | -10.11 cm/s |
| 92817 | Low | No | Yes | No | No | No | No | No | -13.53 cm/s |
| 6255 | Low | No | Yes | No | No | No | No | No | -10.92 cm/s |
| 11850 | Low | No | No | No | No | No | No | No | -9.61 cm/s |
| 94154 | Low | No | No | No | No | No | No | No | -8.99 cm/s |
| 101715 | Low | No | Yes | No | No | No | No | No | -9.24 cm/s |
| 121864 | Low | No | No | No | No | No | No | No | -13.03 cm/s |
| 13849 | High | Yes | No | Yes | No | Yes | No | No | -3.07 cm/s |
| 441439 | Low | No | No | No | No | No | No | No | -10.24 cm/s |
| 64960 | Low | No | No | No | No | No | No | No | -9.13 cm/s |
| 92283 | Low | No | No | No | No | No | No | No | -8.69 cm/s |
| 5282761 | High | No | No | Yes | No | Yes | No | No | -2.60 cm/s |
| 985 | High | Yes | No | Yes | No | Yes | No | No | -2.77 cm/s |
| 5281 | High | No | No | Yes | No | No | No | No | -2.19 cm/s |
| 18950 | Low | No | Yes | No | No | No | No | No | -9.70 cm/s |
| 441033 | Low | No | Yes | No | No | No | No | No | -9.70 cm/s |
| 445639 | High | No | No | Yes | No | Yes | No | No | -2.60 cm/s |
| 54725318 | Low | No | No | No | Yes | No | No | No | -3.79 cm/s |
| 5459879 | Low | No | No | No | No | No | No | No | -10.32 cm/s |

in estrogen production: aromatase (Aro), ES, and 17βHSD, utilizing molecular docking techniques. The docking findings indicated that all the chosen compounds exhibited varying levels of binding affinity toward the active sites of the three target enzymes, as detailed in Table 5. Molecular interactions, such as hydrogen bonds and hydrophobic contacts, were identified between the bioactive compounds and important residues located within the enzyme binding sites (Table 6). Structural interaction visualizations for all compounds with Aro, ES, and 17βHSD are illustrated in Figures 6-8, respectively. Among the 14 compounds, D-Fructose, diethyl mercaptal, pentaacetate (PubChem CID: 344472) showed the strongest binding affinity across all targets. For aromatase, it achieved a binding energy of -8.0 kcal/mol and a Ki of 0.001 mM, forming a hydrogen bond with Tyr361 and displaying hydrophobic interactions with Gln428, Pro429, and Phe430. Regarding ES, the binding energy was -6.6 kcal/mol (Ki=0.01 mM), involving interactions with Leu450, Phe468, and Tyr445. For 17βHSD, the compound recorded a peak binding affinity of -8.2 kcal/mol and a Ki of 0.0006 mM, establishing critical hydrogen bonds with Ser11 and Gly92, along with several hydrophobic contacts.

## DISCUSSION

Breast cancer is one of the most frequent cancers in women globally, with many being hormone-dependent or Estrogen Receptor-Positive (ER+).[11] These types of cancer depend on estrogen signaling for their growth and development, which makes targeting estrogen biosynthesis and receptor pathways essential for treatment.[12] The integration of IEC and SEC successfully distinguished polysaccharides based on their charge and molecular weight, highlighting their diverse characteristics. The presence of distinct IEC peaks indicates heterogeneity among

**Table 4: Evaluation of drug-likeness and oral bioavailability of selected bioactive compounds from PLE using SwissADME. Parameters include Lipinski's Rule of Five, Veber, Ghose, Egan, and Muegge filters, indicating suitability for systemic circulation and potential as orally active drugs.**

| Pub Chem CID | Lipinski | Ghose | Veber | Egan | Muegge | BS |
|---|---|---|---|---|---|---|
| 344472 | Yes; 0 violation | No; 1 violation: MW>480 | No; 2 violations: Rotors>10, TPSA>140 | No; 1 violation: TPSA>131.6 | No; 2 violations: TPSA>150, Rotors>15 | 0.55 |
| 10954115 | Yes; 0 violation | No; 2 violations: WLOGP<-0.4, MR<40 | Yes | Yes | No; 2 violations: MW<200, XLOGP3<-2 | 0.55 |
| 6027 | Yes; 0 violation | No; 3 violations: MW<160, WLOGP<-0.4, MR<40 | Yes | Yes | No; 2 violations: MW<200, XLOGP3<-2 | 0.55 |
| 5961 | Yes; 0 violation | No; 3 violations: MW<160, WLOGP<-0.4, MR<40 | Yes | Yes | No; 2 violations: MW<200, XLOGP3<-2 | 0.55 |
| 6912 | Yes; 0 violation | No; 3 violations: MW<160, WLOGP<-0.4, MR<40 | Yes | Yes | No; 2 violations: MW<200, XLOGP3<-2 | 0.55 |
| 552347 | Yes; 0 violation | Yes | No; 1 violation: Rotors>10 | Yes | Yes | 0.55 |
| 219893 | Yes; 1 violation: NHorOH>5 | No; 1 violation: WLOGP<-0.4 | No; 1 violation: TPSA>140 | No; 1 violation: TPSA>131.6 | No; 2 violations: XLOGP3<-2, H-don>5 | 0.55 |
| 76599 | Yes; 1 violation: NHorOH>5 | No; 1 violation: WLOGP<-0.4 | Yes | No; 1 violation: TPSA>131.6 | No; 2 violations: XLOGP3<-2, H-don>5 | 0.55 |
| 92817 | No; 3 violations: MW>500, NorO>10, NHorOH>5 | No; 2 violations: MW>480, WLOGP<-0.4 | No; 1 violation: TPSA>140 | No; 1 violation: TPSA>131.6 | No; 4 violations: XLOGP3<-2, TPSA>150, H-acc>10, H-don>5 | 0.17 |
| 6255 | No; 2 violations: NorO>10, NHorOH>5 | No; 1 violation: WLOGP<-0.4 | No; 1 violation: TPSA>140 | No; 1 violation: TPSA>131.6 | No; 4 violations: XLOGP3<-2, TPSA>150, H-acc>10, H-don>5 | 0.17 |
| 11850 | Yes; 1 violation: NHorOH>5 | No; 2 violations: WLOGP<-0.4, MR<40 | Yes | Yes | No; 3 violations: MW<200, XLOGP3<-2, H-don>5 | 0.55 |
| 94154 | Yes; 0 violation | No; 3 violations: MW<160, WLOGP<-0.4, MR<40 | Yes | Yes | No; 2 violations: MW<200, XLOGP3<-2 | 0.55 |
| 101715 | Yes; 0 violation | No; 2 violations: WLOGP<-0.4, MR<40 | Yes | Yes | No; 2 violations: MW<200, XLOGP3<-2 | 0.55 |
| 121864 | Yes; 1 violation: NHorOH>5 | No; 1 violation: WLOGP<-0.4 | No; 2 violations: Rotors>10, TPSA>140 | No; 1 violation: TPSA>131.6 | No; 3 violations: XLOGP3<-2, TPSA>150, H-don>5 | 0.55 |
| 13849 | Yes; 0 violation | Yes | No; 1 violation: Rotors>10 | Yes | No; 1 violation: XLOGP3>5 | 0.85 |
| 441439 | Yes; 1 violation: NHorOH>5 | No; 1 violation: WLOGP<-0.4 | No; 1 violation: TPSA>140 | No; 1 violation: TPSA>131.6 | No; 2 violations: XLOGP3<-2, H-don>5 | 0.55 |

| Pub Chem CID | Lipinski | Ghose | Veber | Egan | Muegge | BS |
|---|---|---|---|---|---|---|
| 64960 | Yes; 0 violation | No; 2 violations: WLOGP<-0.4, MR<40 | Yes | Yes | No; 2 violations: MW<200, XLOGP3<-2 | 0.55 |
| 92283 | Yes; 0 violation | No; 2 violations: WLOGP<-0.4, MR<40 | Yes | Yes | No; 1 violation: MW<200 | 0.55 |
| 5282761 | Yes; 1 violation: MLOGP>4.15 | No; 1 violation: WLOGP>5.6 | No; 1 violation: Rotors>10 | No; 1 violation: WLOGP>5.88 | No; 1 violation: XLOGP3>5 | 0.85 |
| 985 | Yes; 1 violation: MLOGP>4.15 | Yes | No; 1 violation: Rotors>10 | Yes | No; 1 violation: XLOGP3>5 | 0.85 |
| 5281 | Yes; 1 violation: MLOGP>4.15 | No; 1 violation: WLOGP>5.6 | No; 1 violation: Rotors>10 | No; 1 violation: WLOGP>5.88 | No; 2 violations: XLOGP3>5, Rotors>15 | 0.85 |
| 18950 | Yes; 0 violation | No; 2 violations: WLOGP<-0.4, MR<40 | Yes | Yes | No; 2 violations: MW<200, XLOGP3<-2 | 0.55 |
| 441033 | Yes; 0 violation | No; 2 violations: WLOGP<-0.4, MR<40 | Yes | Yes | No; 2 violations: MW<200, XLOGP3<-2 | 0.55 |
| 445639 | Yes; 1 violation: MLOGP>4.15 | No; 1 violation: WLOGP>5.6 | No; 1 violation: Rotors>10 | No; 1 violation: WLOGP>5.88 | No; 1 violation: XLOGP3>5 | 0.85 |
| 54725318 | Yes; 0 violation | No; 1 violation: #atoms>70 | No; 1 violation: Rotors>10 | Yes | No; 2 violations: XLOGP3>5, Rotors>15 | 0.56 |
| 5459879 | Yes; 1 violation: NHorOH>5 | No; 1 violation: WLOGP<-0.4 | Yes | No; 1 violation: TPSA>131.6 | No; 2 violations: XLOGP3<-2, H-don>5 | 0.55 |

the polysaccharides, aligning with earlier research on fungal polysaccharides. The SEC analysis revealed a majority of high molecular weight polysaccharides, which are typically associated with enhanced bioactivities, including immunomodulatory and antioxidant properties. These findings underscore the significance of utilizing both charge- and size-based methods to isolate biologically active polysaccharide fractions.[13]

The progression of HDBC is closely linked with the localized synthesis and regulation of estrogens in tumor tissues. Three critical enzymes aromatase, ES, and 17βHSD be fundamental to the intracrine production of active estrogens from circulating precursors.[14] Targeting these enzymes offers a promising therapeutic approach to lower estrogen levels and inhibit cancer growth. Our research examined the ability of PLE to inhibit these enzymes, demonstrating significant suppression of enzyme activity across all three targets.[15] Aromatase converts androgens to estrogens and is often overexpressed in breast tumors, thereby enhancing local estrogen production.[16] PLE showed considerable inhibition of aromatase, suggesting the presence of compounds that can block the conversion of androgens to estrogens, potentially limiting estrogen availability in the breast cancer environment.[17] ES hydrolyzes inactive estrogen sulfates into active estrogens, which helps replenish the estrogen pool within tumors.[18] The inhibition of ES by PLE signifies an additional mechanism to regulate estrogen levels, working alongside aromatase inhibition to further diminish estrogenic stimulation of cancer cells.[19] 17βHSD manages the conversion between estrone and the more active E2.[20] By inhibiting 17βHSD, the production of E2, the most biologically active form of estrogen that promotes breast cancer cell proliferation, is reduced.[21] Our findings revealed strong inhibition of 17βHSD activity by PLE, comparable to standard inhibitors, suggesting a significant potential to decrease local E2 levels.[22] The combined inhibition of these three enzymes by PLE indicates a multi-target strategy for disrupting estrogen biosynthesis and metabolism in HDBC. This is particularly advantageous since reliance on single-enzyme inhibition can be evaded through alternative estrogen synthesis pathways. The polypharmacological nature of PLE may thus enhance effectiveness and lower the risk of developing resistance.[23]

PLE shows substantial inhibitory effects on aromatase, ES, and 17βHSD, underscoring its potential as a natural source of multi-target inhibitors for treating hormone-dependent

**Table 5: Binding affinities and estimated inhibition constants (Ki) of selected bioactive compounds from PLE against key estrogen biosynthesis enzymes (aromatase, estrone sulfatase, and 17βHSD) determined by molecular docking.**

| Pub Chem CID | Target Enzymes | Binding energy (kcal/mol) | Ki (μM) | pKm |
|---|---|---|---|---|
| 5961 | Aro | -4.9 | 0.26 | 3.59 |
| 5961 | ES | -4.8 | 0.30 | 3.52 |
| 5961 | 17βHSD | -5.4 | 0.11 | 3.96 |
| 6027 | Aro | -4.9 | 0.26 | 3.59 |
| 6027 | ES | -4.8 | 0.30 | 3.52 |
| 6027 | 17βHSD | -5.2 | 0.15 | 3.81 |
| 6912 | Aro | -4.4 | 0.60 | 3.23 |
| 6912 | ES | -4.6 | 0.42 | 3.37 |
| 6912 | 17βHSD | -5.1 | 0.18 | 3.74 |
| 13849 | Aro | -6.1 | 0.03 | 4.47 |
| 13849 | ES | -6.1 | 0.03 | 4.47 |
| 13849 | 17βHSD | -7.5 | 0.003 | 5.50 |
| 18950 | Aro | -5.1 | 0.18 | 3.74 |
| 18950 | ES | -5.6 | 0.08 | 4.10 |
| 18950 | 17βHSD | -5.8 | 0.06 | 4.25 |
| 64960 | Aro | -4.9 | 0.26 | 3.59 |
| 64960 | ES | -5.5 | 0.09 | 4.03 |
| 64960 | 17βHSD | -5.4 | 0.11 | 3.96 |
| 92283 | Aro | -5.4 | 0.11 | 3.96 |
| 92283 | ES | -5.4 | 0.11 | 3.96 |
| 92283 | 17βHSD | -5.6 | 0.08 | 4.10 |
| 94154 | Aro | -4.5 | 0.50 | 3.30 |
| 94154 | ES | -4.9 | 0.26 | 3.59 |
| 94154 | 17βHSD | -5.1 | 0.18 | 3.74 |
| 101715 | Aro | -4.5 | 0.50 | 3.30 |
| 101715 | ES | -5.4 | 0.11 | 3.96 |
| 101715 | 17βHSD | -5.1 | 0.18 | 3.74 |
| 344472 | Aro | -8.0 | 0.001 | 5.86 |
| 344472 | ES | -6.6 | 0.01 | 4.84 |
| 344472 | 17βHSD | -8.2 | 0.00 | 6.01 |
| 441033 | Aro | -6.0 | 0.04 | 4.40 |
| 441033 | ES | -5.5 | 0.09 | 4.03 |
| 441033 | 17βHSD | -5.4 | 0.11 | 3.96 |
| 552347 | Aro | -4.4 | 0.60 | 3.23 |
| 552347 | ES | -5.1 | 0.18 | 3.74 |
| 552347 | 17βHSD | -5.7 | 0.07 | 4.18 |
| 10954115 | Aro | -4.8 | 0.30 | 3.52 |
| 10954115 | ES | -4.7 | 0.36 | 3.45 |
| 10954115 | 17βHSD | -5.1 | 0.18 | 3.74 |
| 54725318 | Aro | -4.1 | 0.99 | 3.01 |
| 54725318 | ES | -4.2 | 0.83 | 3.08 |
| 54725318 | 17βHSD | -6.2 | 0.03 | 4.54 |

**Table 6: Hydrogen bonding and hydrophobic interactions between selected bioactive compounds from PLE and the active sites of key estrogen biosynthesis enzymes (aromatase, estrone sulfatase, and 17βHSD) as determined by molecular docking.**

| Pub Chem CID | Target Enzymes | Hydrogen Bond Interactions | Hydrophobic Interactions |
|---|---|---|---|
| 5961 | Aro | Gln428 | Pro429, Tyr361, Phe427, Val422,Tyr424, Lys440 and Phe432 |
| 5961 | ES | Val347, Gly358 and Gly359 | Asn479,Ile356 and Asn361 |
| 5961 | 17βHSD | Gly9, Gly92, Ser12 and Arg37 | Ser11 and Asp38 |
| 6027 | Aro | Met374, Leu372 and Arg115 | Val373, Phe134, Leu477 and Val370 |
| 6027 | ES | Phe441, His537, Asp422 and His439 | Phe443, Tyr87,Ile420 and Arg424 |
| 6027 | 17βHSD | Ala170, Val178, His179 and Pro249 | Leu174, Leu180, Thr250 and Lys248 |
| 6912 | Aro | Ile133, Ile132, Arg115 and Arg435 | Ala438, Cys437 and Arg145 |
| 6912 | ES | Leu234, Asp169, Lys171, Glu174 and Gly175 | Pro172, Gly173 and Ser176 |
| 6912 | 17βHSD | Ser11, Gly9, Gly92, Asn90, Gly15 and Ser12 | Ile14 and Gly13 |
| 13849 | Aro | - | Asp348, Ile350, Pro429, Lys440, Phe430, Gln428, Tyr361, Tyr441, Gln351 and Ile347 |
| 13849 | ES | - | Leu185, Thr99, Leu103, His346, Lys368, His485 and Val177 |
| 13849 | 17βHSD | Glu282 and His221 | Phe192, Gly92, Leu149, Met279, Val283, Tyr218,Tyr155 and Gly94 |
| 18950 | Aro | Tyr361, Gln428, Gly431 and Lys440 | Tyr441, Phe427, Tyr424, Pro429 and Phe430 |
| 18950 | ES | Thr276, Leu331, Asp334, Asn28 and Arg26 | Pro279, Glu277, Pro27 andThr278, |
| 18950 | 17βHSD | Gly92, Asn90, Gly9, Ser11 and Ser12 | Thr190 and Ala91 |
| 64960 | Aro | Arg192, Gln218 and Glu483 | Asp222, Phe221, His480 and Val313 |
| 64960 | ES | Glu174, Lys171, Arg238, Leu234, Asp169 and Gly175 | Phe237, Gly173, Pro172 and Ser176 |
| 64960 | 17βHSD | Ser12, Ser11, Gly9, Gly92 and Asn90 | Ala91 |
| 92283 | Aro | Arg192, Ser478, Glu483, Asp222 and His480 | Val313, Gln218, Phe221 and Asp309 |
| 92283 | ES | Leu331, Asn28, Arg26 and Asp334 | Arg330, Thr278, Pro279 and Pro27 |
| 92283 | 17βHSD | Asn90,Gly15, Gly9, Ser11 and Ser12 | Ile14 and Gly13 |
| 94154 | Aro | Ala438, Arg145, Ile132, Arg435, Ile133 and Arg115 | Cys437 and Trp141 |
| 94154 | ES | Glu174, Gly173, Gly175, Asp169, Leu234, Arg238 and Lys171 | Pro172, Phe237, Ser176 and Arg168 |
| 94154 | 17βHSD | Ser11, Ser12, Gly15, Asn90, Gly92 and Gly9 | Gly13 |
| 101715 | Aro | Leu372, Met374 and Leu477 | Phe134, Ile133,Val370, Arg115 and Val373 |
| 101715 | ES | Gly173, Gly175, Asp169, Leu234 and Arg238 | Pro172, Phe237 and Ser176 |
| 101715 | 17βHSD | Asn152, Tyr218, Ser222, Lys223 and Met193 | Leu96, Val196, Phe226 and Val225 |
| 344472 | Aro | Tyr361 | Gln428, Pro429, Phe430, Lys440, Tyr424, Tyr441, Glu357 |

| Pub Chem CID | Target Enzymes | Hydrogen Bond Interactions | Hydrophobic Interactions |
|---|---|---|---|
| 344472 | ES | Leu450 | Phe468, Tyr445, Ala448, Thr538, Leu541, Trp96 and Tyr449 |
| 344472 | 17βHSD | Ser11 and Gly92 | Thr41, Asp38, Arg37, Leu36, Gly9, Asn90, Ala91, Ser12 and Leu93 |
| 441033 | Aro | Arg145, Gly436, Arg435, Ile132, Ile133 and Arg115 | Cys437 and Ala438 |
| 441033 | ES | Asp169, Gly175, Arg238, Leu234 and Gly173 | Ser176, Pro172, Lys171 and Phe237 |
| 441033 | 17βHSD | Gly92, Gly9, Ser12, Asn90 and Gly15 | Ala91 and Gly31 |
| 552347 | Aro | Phe427 and Tyr361 | Val445, Tyr441, Pro429, Tyr424, Val422, Met444 and Leu157 |
| 552347 | ES | His439, Phe441, Asp422, His537 and Arg90 | Glu532, Ala533, Phe443, Ile420 and Tyr87 |
| 552347 | 17βHSD | Ser11, Ser12, Gly9, Gly15 and Asn90 | Cys185, Ile14, Met193, Tyr155, Gly13 and Thr190 |
| 10954115 | Aro | Arg403, Arg400, Arg79 and Asn75 | Gly399, Pro368, His475 and Leu479 |
| 10954115 | ES | Asp422, His439, Asp438, Glu440 and Phe441 | Tyr87, Arg424 and Leu442 |
| 10954115 | 17βHSD | Gly92, Gly9, Ser11, Ser12, Gly15 and Asn90 | Ala91, Ile14 and Gly13 |
| 54725318 | Aro | Gln428, Lys440 and Tyr361 | Phe430, Pro429, Tyr424, Tyr441, Phe432, Lys108 and Asn 110 |
| 54725318 | ES | Phe 441, Tyr87 and His537 | Phe443, Arg424, Asp 438, Glu532, Ala533, Asp422 |
| 54725318 | 17βHSD | Gly92, Asn90, Ser12, Gly15 and Gly9 | Thr140, Gly186, Ile14, Val188, Cys185, Ser142, Phe192, Met193, Val196, Leu96, Tyr155, Asn152, Leu149 and Gly13 |

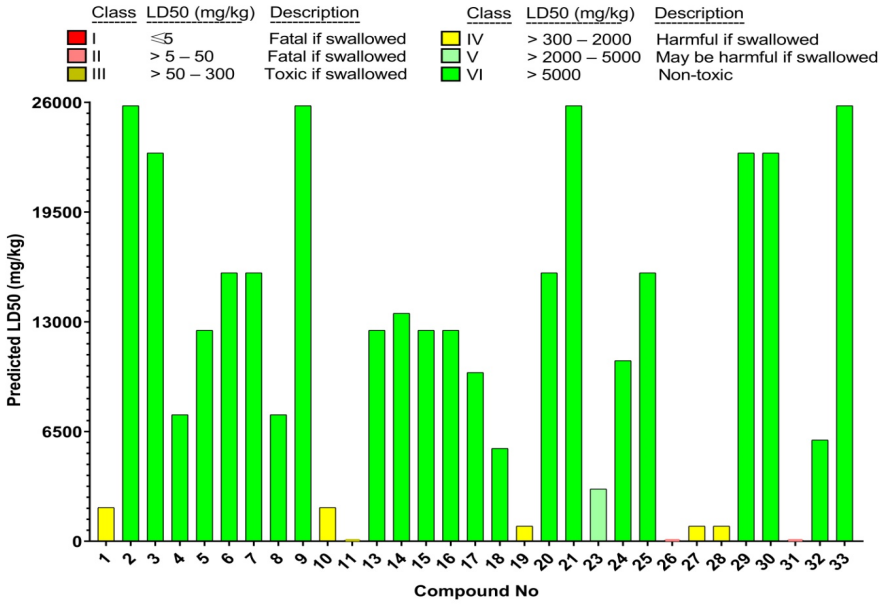


**Figure 5:** Predicted oral toxicity classification of bioactive compounds identified in the PLE. Toxicity was estimated using in silico tools, expressed as median lethal dose ($LD_{50}$, mg/kg), and categorized according to standard toxicity classes. Out of 31 compounds analyzed, 74.2% were assigned to Class 6 (relatively non-toxic; $LD_{50}$ > 5000 mg/kg), one compound to Class 5 (low toxicity), five compounds to Class 4 (moderate toxicity), one compound to Class 3, and two compounds to Class 2 (higher toxicity). The distribution highlights that the majority of compounds in PLE exhibit a favorable safety profile, supporting their potential for pharmaceutical or nutraceutical applications.

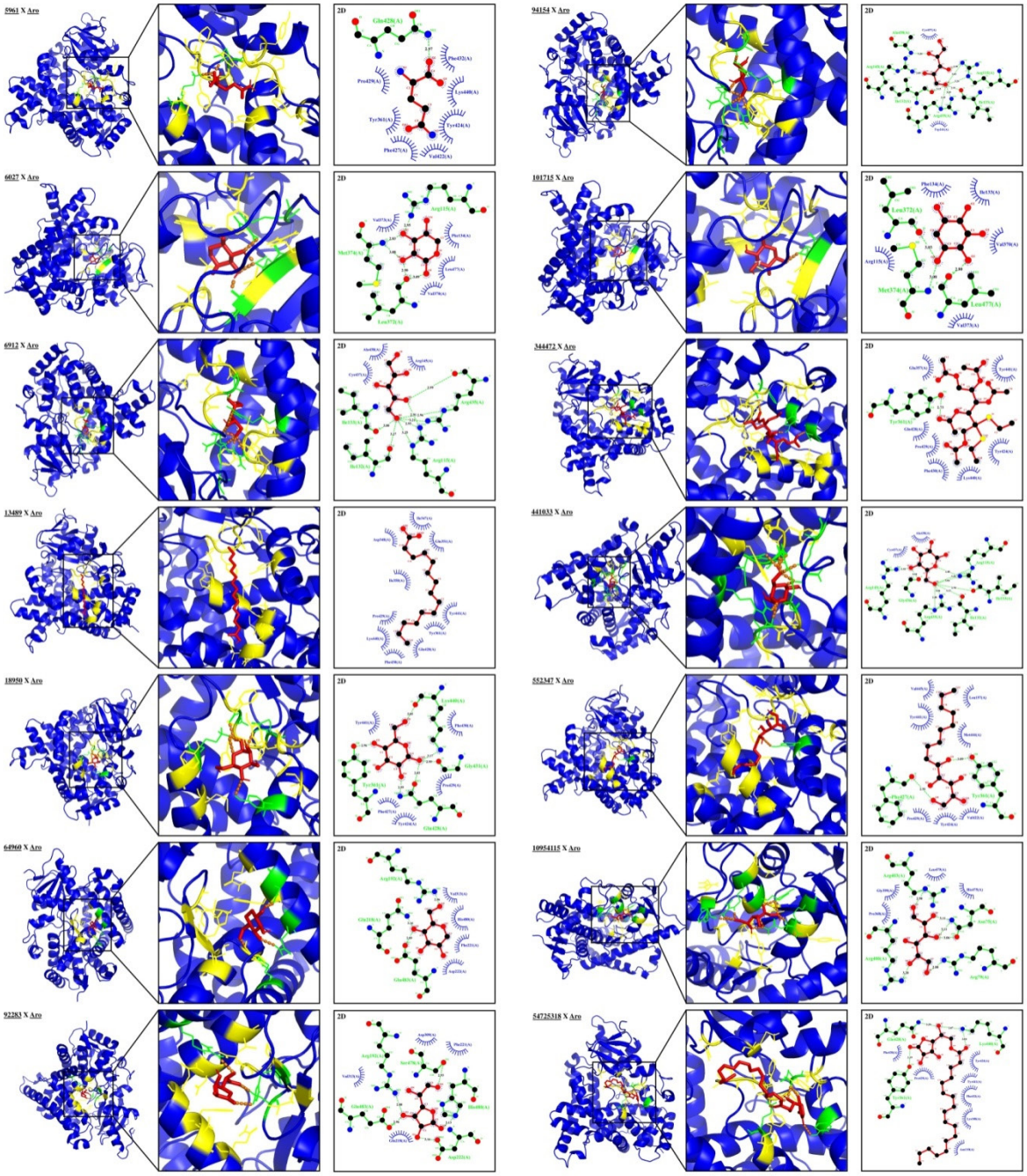

**Figure 6:** Two-dimensional (2D) and three-dimensional (3D) interaction analyses of selected bioactive compounds derived from PLE with the active site of the aromatase (Aro) enzyme. Docking simulations revealed that several compounds displayed strong binding affinities, with D-Fructose, diethyl mercaptal, pentaacetate showing the highest affinity (-8.0 kcal/mol, Ki=0.001 mM). Key interactions included hydrogen bonding with Tyr361 and hydrophobic contacts with Gln428, Pro429, and Phe430, suggesting effective inhibition of Aro activity.

breast cancer. These results warrant further investigation of PLE as an adjunct to endocrine therapy strategies. The screening of pharmacokinetics plays an essential role in identifying potential therapeutic agents by confirming that the compounds have appropriate physicochemical characteristics for drug development.[24] Among the 31 compounds evaluated, 14 were chosen in accordance with key drug-likeness principles, including Lipinski's Rule of Five, along with the Veber, Ghose, Egan, and Muegge benchmarks. These criteria take into account aspects such as molecular weight, the number of hydrogen bond donors and acceptors, lipophilicity (logP), and polar surface area, which suggest a strong potential for oral bioavailability and advantageous drug-like characteristics.

Overall, molecular docking analysis demonstrated that most bioactive compounds from PLE exhibited favorable binding

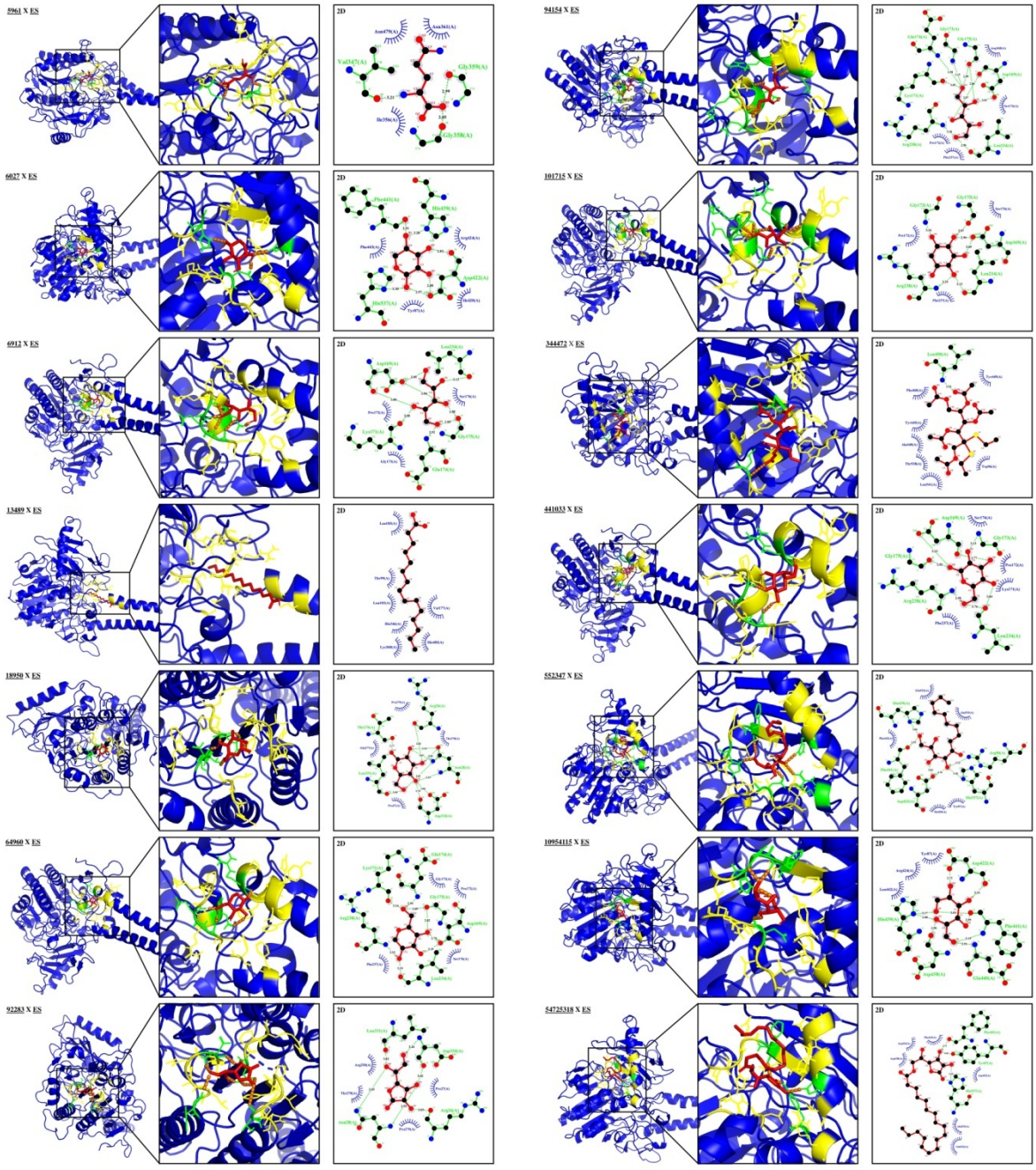

**Figure 7:** Two-dimensional (2D) and three-dimensional (3D) molecular interaction profiles of PLE-derived compounds with Estrogen Synthase (ES). Docking results indicated that the bioactive compounds formed stable interactions within the ES catalytic pocket, with the strongest candidate exhibiting a binding energy of -6.6 kcal/mol (Ki=0.01 mM). Notable interactions involved Leu450, Phe468, and Tyr445, highlighting the compound's potential to disrupt estrogen biosynthesis through ES inhibition.

affinities with aromatase, ES, and 17βHSD. Among the tested candidates, D-Fructose, diethyl mercaptal, pentaacetate showed the most consistent and strongest interactions across all three enzymes, suggesting its potential as a broad-spectrum estrogen biosynthesis inhibitor. These findings highlight the multi-target inhibitory capacity of PLE compounds, reinforcing their therapeutic promise in HDBC.

Aromatase is a cytochrome P450 enzyme that converts androgens to estrogens. In postmenopausal women, the adrenal glands, muscle, and adipose tissue are the main estrogen sources.[25] The use of aromatase inhibitors, which block this pathway and lower estrogen levels, is an essential part of treating HDBC. The strong binding affinity observed for D-Fructose, diethyl mercaptal, pentaacetate suggests that it may operate through a unique interaction profile, with a combination of hydrogen bonding and hydrophobic contacts. This is in contrast to traditional synthetic

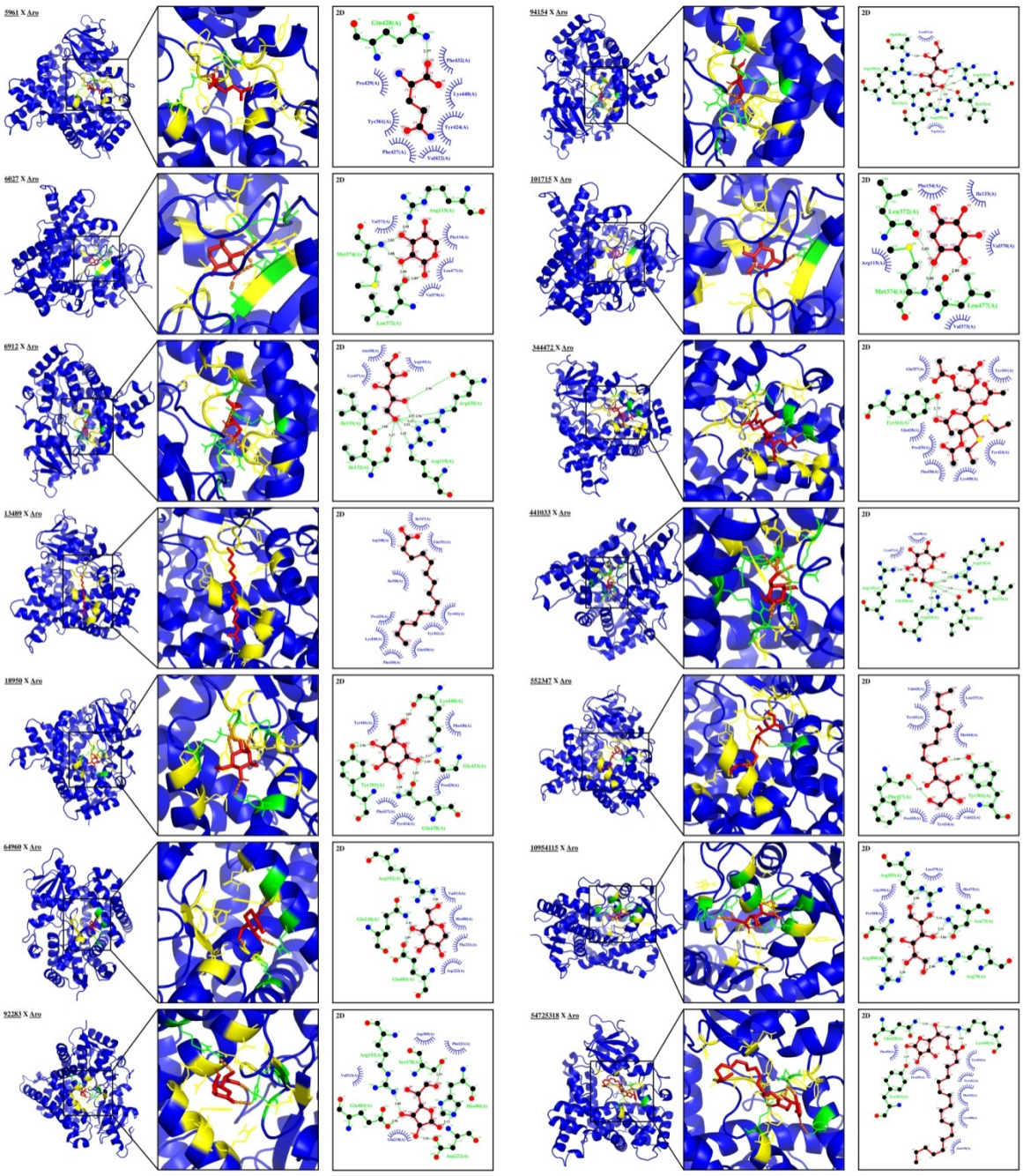

**Figure 8:** Two-dimensional (2D) and three-dimensional (3D) docking interaction analysis of bioactive compounds from PLE with 17βHSD. Among the screened compounds, D-Fructose, diethyl mercaptal, pentaacetate (CID: 344472) demonstrated the highest affinity (-8.2 kcal/mol, Ki=0.0006 mM). The compound formed hydrogen bonds with Ser11 and Gly92, alongside multiple hydrophobic interactions, indicating strong inhibitory potential against 17βHSD, a key regulator in estrogen metabolism.

inhibitors, which typically use a non-steroidal structure to target the heme group of Aromatase. Given its distinct mechanism of action, this compound could offer a more targeted inhibition of Aromatase, potentially reducing off-target effects compared to long-term use of current synthetic inhibitors.

ES plays a critical role in the conversion of estrone sulfate into estrone, which is then converted to E2, a potent estrogen that promotes tumor growth in HDBC. Notably, while Aromatase inhibitors primarily target the conversion of androgens to estrogens, they do not effectively reduce plasma estrone levels. This highlights the need for alternative therapeutic strategies that target ES, particularly in tumors where local estrogen production from estrone sulfate serves as an alternative route for estrogen synthesis.[26,27] The compound's distinct inhibition of ES through the combination of hydrophobic and hydrogen bonding interactions provides a strong binding profile that may offer advantages over other steroidal and non-steroidal ES inhibitors,

which often face issues with selectivity and potency. Given the ability of D-Fructose, diethyl mercaptal, pentaacetate to modulate this alternative estrogen production pathway, it may be valuable addition to current treatment options, particularly when combined with Aro inhibitors. This dual inhibition approach could enhance estrogen suppression in hormone-dependent cancers, potentially overcoming the limitations of current monotherapies.

17βHSD is critical in the local biosynthesis of E2, a potent estrogen that promotes breast cancer progression. Overexpression of 17βHSD in breast cancer tissues leads to elevated intratumoral E2 concentrations, which drives tumor growth. However, in malignant tissues, decreased expression of 17βHSD2 prevents E2 from being converted to estrone, which raises E2 levels and accelerates tumor growth.[28,29] Inhibiting 17βHSD thus emerges as a promising strategy to reduce intratumoral estrogen levels and suppress tumor progression. The inhibition of 17βHSD by D-Fructose, diethyl mercaptal, pentaacetate is particularly significant because it may reduce estrogenic signaling while potentially favoring the increase of androgenic inhibition of tumor growth. This is particularly important for breast cancer, as tumor development is significantly influenced by local estrogen production. The compound's distinct molecular interaction profile, which differs from those of traditional steroidal and non-steroidal inhibitors of 17βHSD, suggests that it could offer a more specific and potent alternative to existing therapies. Given that 17βHSD inhibitors could reduce estrogen levels while potentially enhancing androgenic inhibition of tumor growth, D-Fructose, diethyl mercaptal, pentaacetate shows promising therapeutic potential along with other agents targeting estrogen biosynthesis pathways.

These tumors rely on estrogens for their growth and progression and are categorized as hormone-dependent breast cancers. Estrogens, especially E2, improve the propagation and survival of breast cancer cells by binding to ERs, which activates transcriptional pathways that control the cell cycle, apoptosis, and metastasis.[12] Specifically, E2 plays an essential role in estrogen-dependent breast cancer, with higher concentrations in breast tumors than in plasma. Critical enzymes involved in estrogen production, such as aromatase, ES, and 17β-hydroxysteroid dehydrogenase, facilitate the conversion of androgens to estrogens, and the transformation of estrone to E2, which triggers tumor cell growth.[30] Extended exposure to estrogen, influenced by factors such as early menopause, age at first childbirth, and childbearing age, increases the risk of breast cancer. Consequently, targeting estrogen production through enzyme inhibition represents a shows potential therapeutic approach for HDBC.[4]

## CONCLUSION

In conclusion, this study demonstrates that PLE and its bioactive compounds effectively inhibit key estrogen biosynthesis enzymes aromatase, ES, and 17βHSD in a dose-dependent manner. Among these, D-fructose diethyl mercaptal pentaacetate emerged as a potent multi-target inhibitor with strong binding affinities. These findings highlight the potential of PLE as a natural candidate for regulating estrogen production in HDBC. Further preclinical and clinical studies are warranted to confirm its safety and therapeutic applicability.

## ACKNOWLEDGEMENT

The authors wish to acknowledge the Indian Council of Medical Research, Government of India, for their financial support of this research (Grant No: ISRM/12(27)/2020; dated 01.09.2020). Authors also extend their gratitude to the management of K.S. Rangasamy College of Arts and Science (Autonomous), Tiruchengode, Tamil Nadu, India, for providing the essential infrastructure.

## FUNDING

This research was financially supported by the Indian Council of Medical Research, Government of India, New Delhi (Project Ref No: ISRM/12(27)/2020, dated 01.09.2020).

## CONFLICT OF INTEREST

The authors declare that there is no Conflict of Interest.

## ABBREVIATIONS

**ES:** Estrone sulfatase; **17βHSD:** 17β-Hydroxysteroid dehydrogenase; **ADME:** Absorption, distribution, metabolism, and excretion; **ES:** 17β-Estradiol; **L. edodes:** *Lentinula edodes*; **PLE:** Partially Purified Polysaccharides from *Lentinula edodes*; **TNAU:** Tamil Nadu Agricultural University; **IEC:** Ion exchange chromatography; **SEC:** Size-exclusion chromatography; **ELISA:** Enzyme-Linked Immunosorbent Assay; **OD:** Optical Density; **GC-MS:** Gas Chromatography Mass Spectrophotometry; **Ki:** Inhibition constant; **ER+:** Estrogen receptor-positive; **HDBC:** Hormone dependent breast cancer; **BS:** Bioavailability Score.

## SUMMARY

This study explored the potential of PLE as natural inhibitors of enzymes critical to estrogen biosynthesis aromatase, ES, and 17βHSD which are central to HDBC progression. Polysaccharide fractions were purified through ion-exchange and size-exclusion chromatography, and enzyme inhibition assays demonstrated potent, dose-dependent effects, with inhibition exceeding 86% at 400 µg/mL. The $IC_{50}$ values further confirmed strong activity against all three targets. GC-MS profiling identified 33 bioactive metabolites, of which 14 underwent pharmacokinetic and

toxicity evaluation using SwissADME and ProTox 3.0. Among these, molecular docking studies highlighted D-fructose diethyl mercaptal pentaacetate as the most promising multi-target inhibitor, showing robust binding affinities with aromatase, ES, and 17βHSD. Collectively, these findings indicate that PLE, particularly D-fructose diethyl mercaptal pentaacetate, may serve as a natural, multi-target adjunct to endocrine therapies in HDBC, meriting further mechanistic investigation and preclinical validation.

## REFERENCES


1. International Agency for Research on Cancer, World Health Organization. Global Cancer Observatory. Cancer Today. International Agency for Research on Cancer, World Health Organization; 2023. Accessed March 22, 2025. https://gco.iarc.fr/
2. Kulothungan V, Ramamoorthy T, Sathishkumar K, Mohan R, Tomy N, Miller GJ, *et al.* Burden of female breast cancer in India: estimates of YLDs, YLLs, and DALYs at national and subnational levels based on the national cancer registry programme. Breast Cancer Research and Treatment 2024;205(2):323-32.
3. Jena D, Padhi BK, Zahiruddin QS, Ballal S, Kumar S, Bhat M, *et al.* Estimation of burden of cancer incidence and mortality in India: based on global burden of disease study 1990-2021. BMC Cancer 2024;24(1):1278.
4. Hong Y, Chen S. Aromatase, estrone sulfatase, and 17β-hydroxysteroid dehydrogenase: structure-function studies and inhibitor development. Molecular and Cellular Endocrinology 2011;340(2):120-6.
5. Sathishkumar K, Chaturvedi M, Das P, Stephen S, Mathur P. Cancer incidence estimates for 2022 and projection for 2025: result from National Cancer Registry Programme, India. Indian Journal of Medical Research 2022;156(4&5): 598-607.
6. Ponnusamy C, Uddandrao VVS, Pudhupalayam SP, Singaravel S, Periyasamy T, Ponnusamy P, *et al. Lentinula Edodes* (Edible Mushroom) as a Nutraceutical: A Review. Biosciences Biotechnology Research Asia 2022;19(1).
7. Ponnusamy C, Uddandrao VVS, Sasikumar V, Prabhu P, Ganapathy S. Partially Purified Polysaccharides from Lentinus edodes (Mushroom) Scavenge Free Radicals and Induce Apoptosis in MCF-7 Cancer Cells by Regulating Apoptotic Genes. Indian Journal of Pharmaceutical Education and Research 2024;58(2):535-45.
8. Uddandrao S, Parim B, Saravanan G. Evaluation of the antioxidant and antidiabetic potential of the poly herbal formulation: identification of bioactive factors. Cardiovascular and Hematological Agents in Medicinal Chemistry 2020;18(2):111-23.
9. Banerjee P, Eckert AO, Schrey AK, Preissner R. ProTox-II: a webserver for the prediction of toxicity of chemicals. Nucleic Acids Research 2018; 46(W1):W257-W263.
10. SwissADME: a free web tool to evaluate pharmacokinetics, drug-likeness and medicinal chemistry friendliness of small molecules. Scientific Reports 2017;7:42717.
11. Łukasiewicz S, Czeczelewski M, Forma A, Baj J, Sitarz R, Stanisławek A. Breast Cancer-Epidemiology, Risk Factors, Classification, Prognostic Markers, and Current Treatment Strategies-An Updated Review. Cancers (Basel) 2021;13(17):4287.
12. Miziak P, Baran M, Błaszczak E, Przybyszewska-Podstawka A, Kałafut J, Smok-Kalwat J, *et al.* Estrogen Receptor Signaling in Breast Cancer. Cancers (Basel). 2023;15(19):4689.
13. Dai Y, Wang L, Chen X, Song A, He L, Wang L, *et al. Lentinula edodes* Sing Polysaccharide: Extraction, Characterization, Bioactivities, and Emulsifying Applications. Foods 2023;12(17):3289.
14. Zhao H, Zhou L, Shangguan AJ, Bulun SE. Aromatase expression and regulation in breast and endometrial cancer. Journal of Molecular Endocrinology 2016;57(1):19-33.
15. Bruno RD, Njar VC. Targeting cytochrome P450 enzymes: a new approach in anti-cancer drug development. Bioorganic and Medicinal Chemistry 2007;15(15):5047-60.
16. Chan HJ, Petrossian K, Chen S. Structural and functional characterization of aromatase, estrogen receptor, and their genes in endocrine-responsive and -resistant breast cancer cells. The Journal of Steroid Biochemistry and Molecular Biology 2016;161:73-83.
17. Santen RJ, Yue W, Naftolin F, Mor G, Berstein L. The potential of aromatase inhibitors in breast cancer prevention. Endocrine-Related Cancer 1999;6(2):235-43.
18. Santner SJ, Ohlsson-Wilhelm B, Santen RJ. Estrone sulfate promotes human breast cancer cell replication and nuclear uptake of estradiol in MCF-7 cell cultures. International Journal of Cancer 1993;54(1):119-24.
19. Pasqualini JR, Chetrite GS. Recent insight on the control of enzymes involved in estrogen formation and transformation in human breast cancer. The Journal of Steroid Biochemistry and Molecular Biology 2005;93(2-5):221-36.
20. Gunnarsson C, Hellqvist E, Stål O. 17beta-Hydroxysteroid dehydrogenases involved in local oestrogen synthesis have prognostic significance in breast cancer. British Journal of Cancer 2005;92(3):547-52.
21. Aka JA, Mazumdar M, Chen CQ, Poirier D, Lin SX. 17beta-hydroxysteroid dehydrogenase type 1 stimulates breast cancer by dihydrotestosterone inactivation in addition to estradiol production. Molecular Endocrinology 2010;24(4):832-45.
22. Delvoux B, D'Hooghe T, Kyama C, Koskimies P, Hermans RJ, Dunselman GA, *et al.* Inhibition of type 1 17β-hydroxysteroid dehydrogenase impairs the synthesis of 17β-estradiol in endometriosis lesions. The Journal of Clinical Endocrinology and Metabolism 2014;99(1):276-84.
23. Pasqualini JR. The selective estrogen enzyme modulators in breast cancer: a review. Biochimica et Biophysica Acta 2004;1654(2):123-43.
24. Tuntland T, Ethell B, Kosaka T, Blasco F, Zang RX, Jain M, *et al.* Implementation of pharmacokinetic and pharmacodynamic strategies in early research phases of drug discovery and development at Novartis Institute of Biomedical Research. Frontiers in Pharmacology 2014;5:174.
25. Blakemore J, Naftolin F. Aromatase: Contributions to Physiology and Disease in Women and Men. Physiology (Bethesda) 2016;31(4):258-269.
26. Ghosh D. Structures and functions of human placental aromatase and steroid sulfatase, two key enzymes in estrogen biosynthesis. Steroids 2023;196:109249.
27. Secky L, Svoboda M, Klameth L, Bajna E, Hamilton G, Zeillinger R, *et al.* The sulfatase pathway for estrogen formation: targets for the treatment and diagnosis of hormone-associated tumors. Journal of Drug Delivery Science and Technology 2013: 957605.
28. Xanthoulea S, Konings GFJ, Saarinen N, Delvoux B, Kooreman LFS, Koskimies P, *et al.* Pharmacological inhibition of 17β-hydroxysteroid dehydrogenase impairs human endometrial cancer growth in an orthotopic xenograft mouse model. Cancer Letters 2021;508:18-29.
29. Poirier D. Recent advances in the development of 17beta-hydroxysteroid dehydrogenase inhibitors. Steroids 2025;213:109529.


**Cite this article:** Ponnusamy C, Uddandrao VVS, Sasikumar V, Prabhu P, Ganapathy S. *Lentinula edodes* Polysaccharides Inhibit Estrogen Biosynthesis Enzymes in Hormone-Dependent Breast Cancer. Indian J of Pharmaceutical Education and Research. 2026;60(3s):s1139-s1155.